# Controlling the Numerical Cerenkov Instability in PIC simulations using a customized FDTD Maxwell solver and a local FFT based current correction


Fei Li[a], Peicheng Yu[b], Xinlu Xu[b], Frederico Fiuza[c], Viktor K. Decyk[b], Thamine Dalichaouch[b], Asher Davidson[b], Adam Tableman[b], Weiming An[b], Frank S. Tsung[b], Ricardo A. Fonseca[d,e], Wei Lu[a], Warren B. Mori[b]

[a]Tsinghua University, Beijing 100084, China

[b]University of California Los Angeles, CA 90095, USA

[c]SLAC National Accelerator Laboratory, CA 94025, USA

[d]Instituto Superior Técnico, Lisbon, Portugal

[e]ISCTE - Instituto Universitário de Lisboa, 1649–026, Lisbon, Portugal

# Simulations in plasma-based acceleration

- We rely on Particle-in-cell simulations to give us vision on the physics in plasma-based acceleration
  - Plasma density highly modulated
  - Acceleration field highly nonlinear
  - Particle trajectory highly irregular
  - Subtle physical process

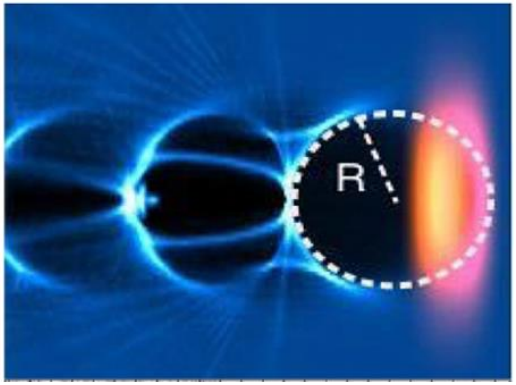


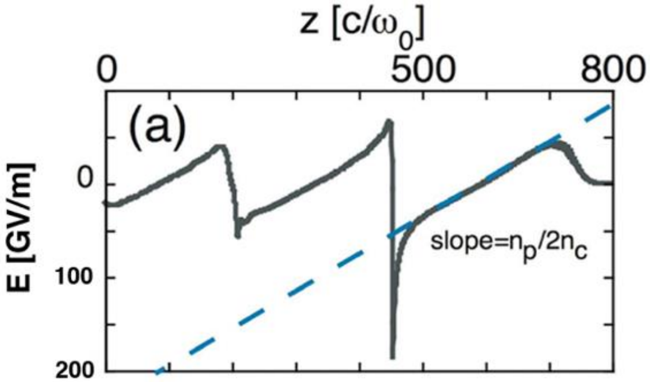


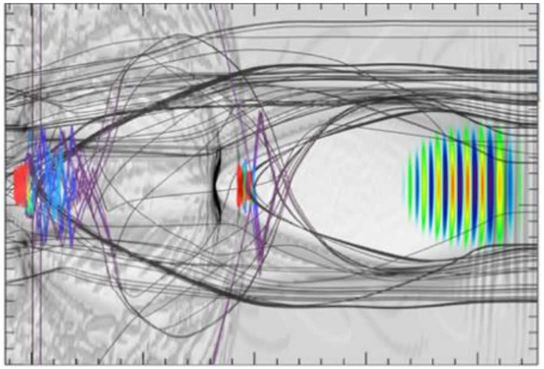

A. Pukhov and J. Meyer-ter-vehn, Appl. Phys. B 74, 355 (2002).
J. B. Rosenzweig, et al., Phys. Rev. A, 44:R6189-92 (1991).
W. Lu, et al., Phys. Rev. Lett. 96, 16502 (2006).

# Particle-in-Cell (PIC)

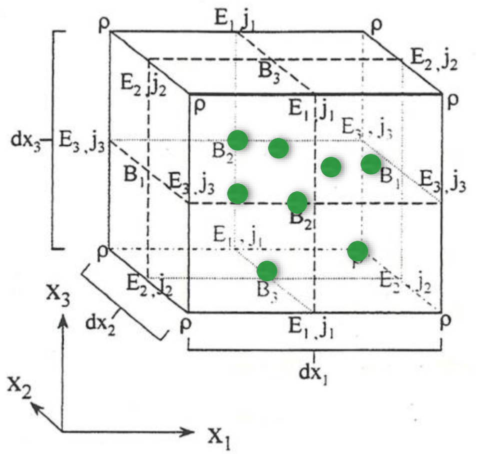

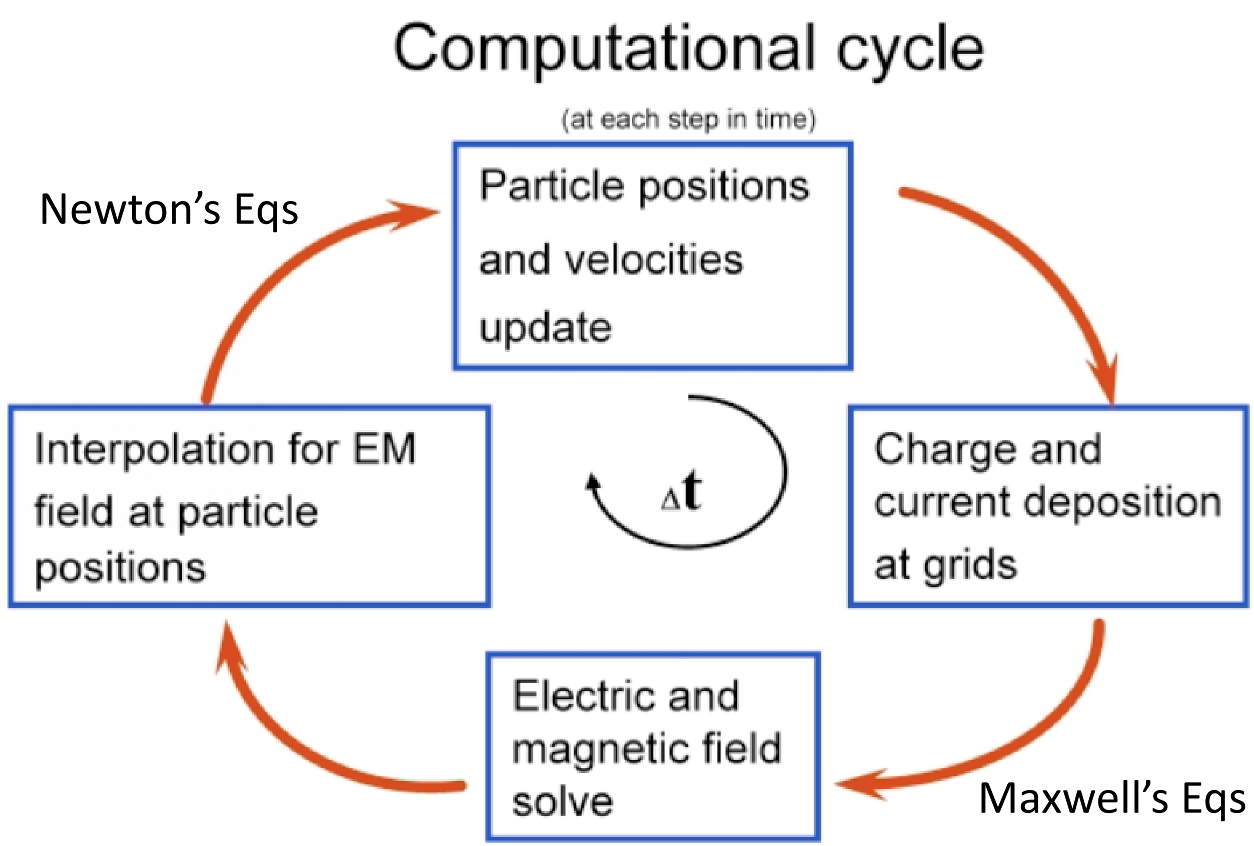



J. Dawson, Review of Modern Physics, Vol. 55, No. 2, April 1983.
C. K. Birdsall, L. A. Bruce, Plasma physics via computer simulations. New York: McGraw-Hill, 1985.

# Numerical Instability in relativistically drifting plasma

LWFA simulation in the Lorentz boosted frame, Numerical Cerenkov Instability (**NCI**)

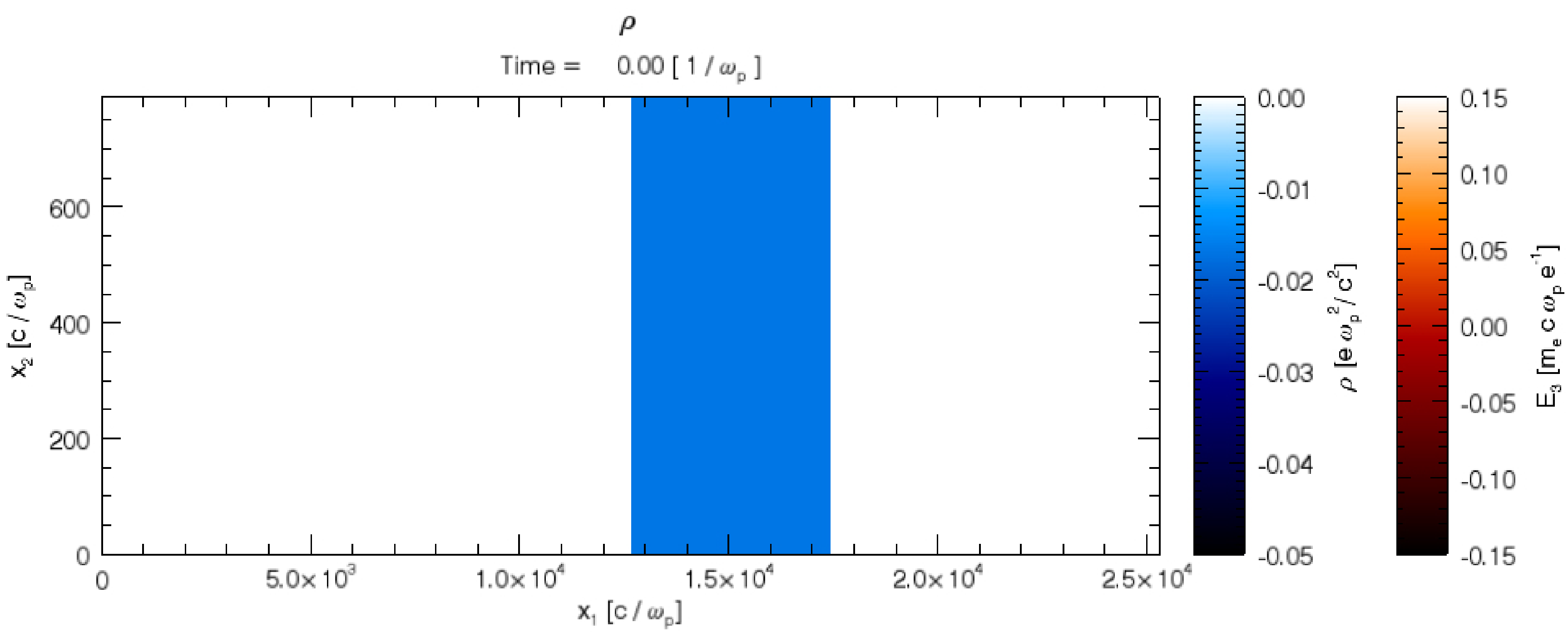


W. Mori, et. al., NSF Proposal (1992).
J.-L. Vay, Phys. Rev. Lett., 98, 130405 (2007).

JOURNAL OF COMPUTATIONAL PHYSICS 15, 504–521 (1974)

Numerical Cherenkov Instabilities in Electromagnetic Particle Codes*

BRENDAN B. GODFREY

*University of California, Los Alamos Scientific Laboratory, Los Alamos, New Mexico 87544*

Received September 11, 1973; revised May 10, 1974

Godfrey, J. Comp. Phys., 15, 504 (1974)

- B. B. Godfrey and J.-L. Vay, J. Comp. Phys. 248, 33-46 (2013).
- J.-L. Vay, I. Haber and B. B. Godfrey, J. Comp. Phys. 243, 260-268 (2013).
- B. B. Godfrey and J.-L. Vay, J. Comp. Phys. 267, 1-6 (2014).
- B. B. Godfrey, J.-L. Vay and I. Haber, J. Comp. Phys. 258, 689-704 (2014).
- B. B. Godfrey and J.-L. Vay, Comp. Phys. Comm. 196, 221-225 (2015).

- P. Yu, X. Xu, et. al, in Proc. 15th AAC Workshop, Austin, TX, 2012.
- X. Xu, P. Yu, et al, Comp. Phys. Comm. 184 (11), 2503-2514 (2013).
- P. Yu, X. Xu, et. al, J. Comp. Phys. 266, 124 (2014).
- P. Yu, X. Xu, et al, Comp. Phys. Comm. 192, 32-47 (2015).
- P. Yu, X. Xu, et al, Comp. Phys. Comm. 197, 144-152 (2015).
- F. Li, P. Yu, et al, arXiv:1605.01496v1

# Theoretical viewpoint

Numerical dispersion relation

$$\left((\omega' - k_1'v_0)^2 - \frac{\omega_p^2}{\gamma^3}(-1)^\mu \frac{S_{j1}S_{E1}\omega'}{[\omega]}\right) \times$$
$$\left([\omega]^2 - [k]_{E1}[k]_{B1} - [k]_{E2}[k]_{B2} - \frac{\omega_p^2}{\gamma}(-1)^\mu \frac{S_{j2}(S_{E2}[\omega] - S_{B3}[k]_{E1}v_0)}{\omega' - k_1'v_0}\right)$$
$$+\mathcal{C} = 0$$

Langmuir mode

$$(\omega - k_1 v_0)^2 - \frac{\omega_p^2}{\gamma^3} = 0$$

EM mode

$$\omega^2 - k_1^2 - k_2^2 - \frac{\omega_p^2}{\gamma} = 0$$

Coupling term

$$\mathcal{C} = \frac{\omega_p^2}{\gamma}\frac{(-1)^\mu}{[\omega]}\Big\{S_{j1}S_{E1}\omega'[k]_{E2}[k]_{B2}(v_0^2 - 1) + S_{j2}S_{E2}[k]_{E2}[k]_{B2}(\omega' - k_1'v_0)$$
$$+ S_{j1}[k]_{E2}(S_{E2}[k]_{B1}k_2v_0 - S_{B3}k_2v_0^2[\omega])\Big\}$$

$\mathcal{C} = 0$ in the continuous limit

X. Xu, et al. Computer Physics Communications 184 (11), 2503-2514 (2013).

# FFT based solver

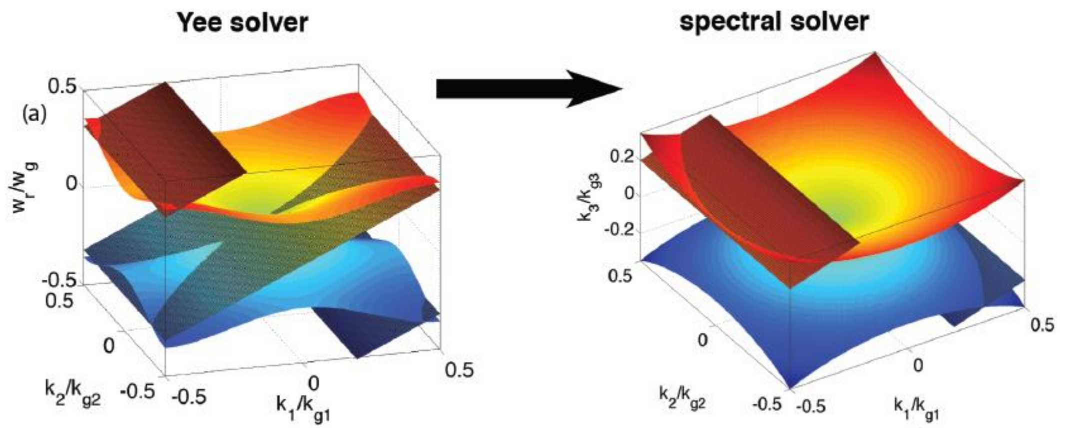


Advantage of FFT based solver

- More localized (0,0) NCI modes.
- Smaller growth rate for (0,0) NCI modes.

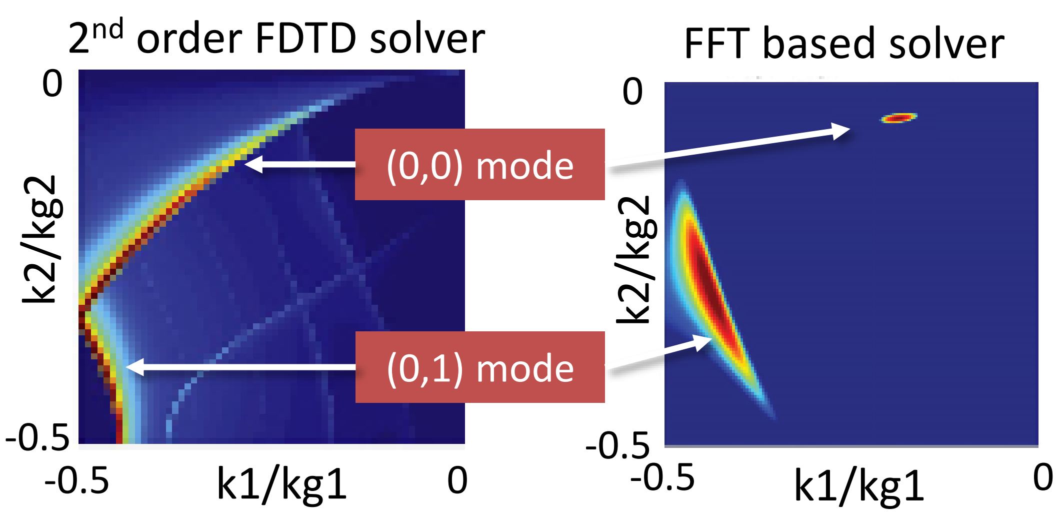


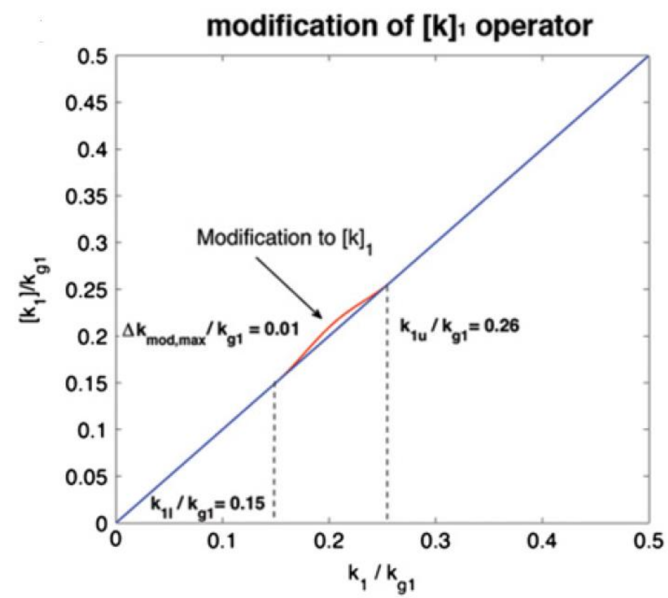


X. Xu, et al, Computer Physics Communications **184** (11), 2503-2514 (2013)
P. Yu, et al, Computer Physics Communications **197**, 144-152 (2015).

# EM field advance for FFT based solver

Parallel scalability

- Global FFT. Single partition in plasma drifting direction

Computing efficiency

- FFT/IFFT pairs frequently used in advancing EM field

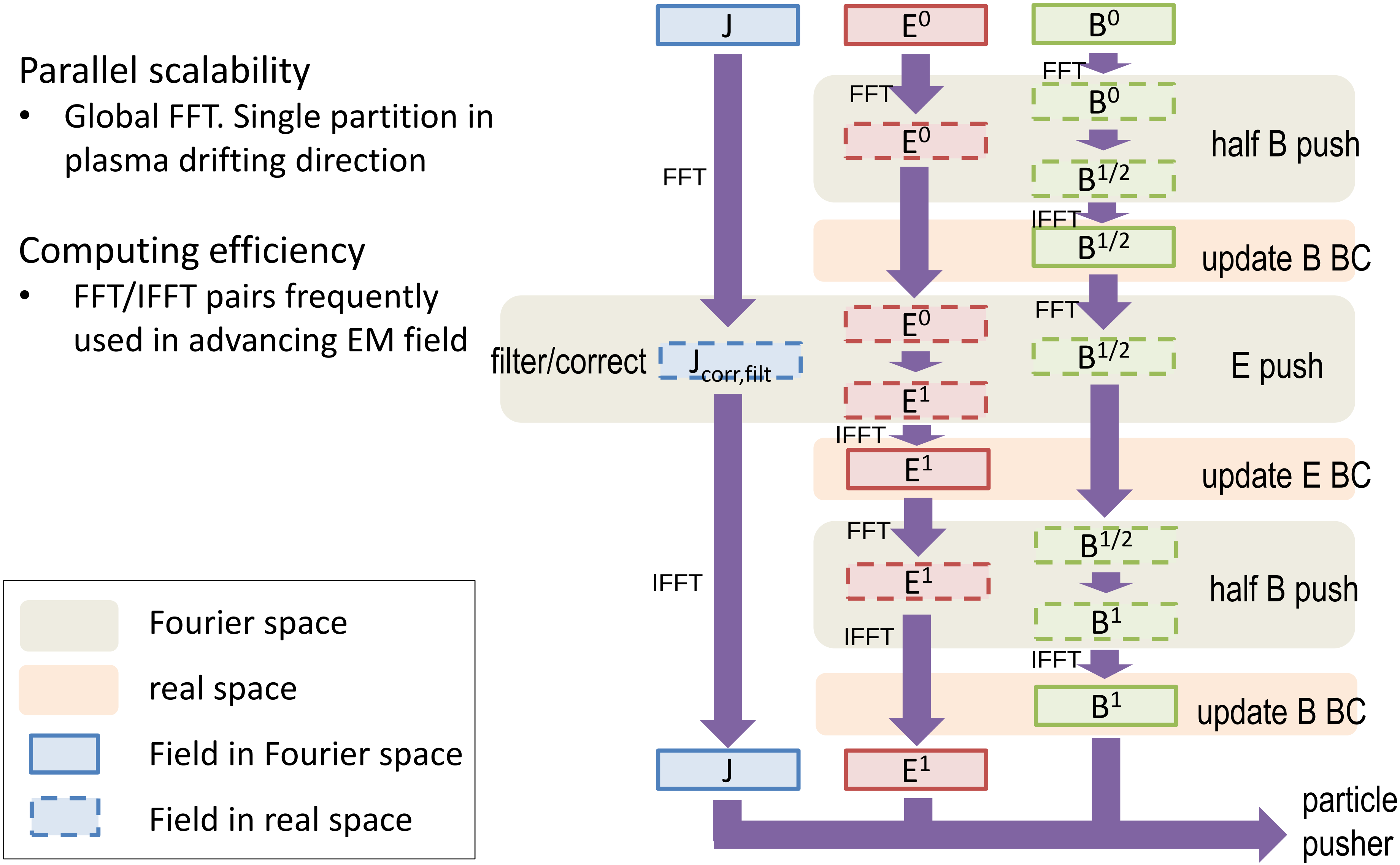

# Numerical dispersion of high-order (HO) FDTD solver

ω-k relation

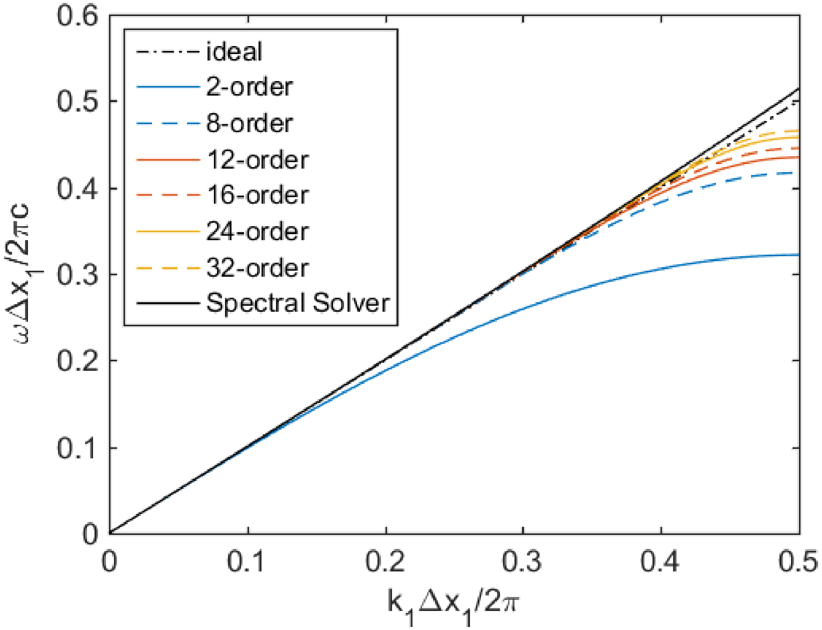


phase velocity

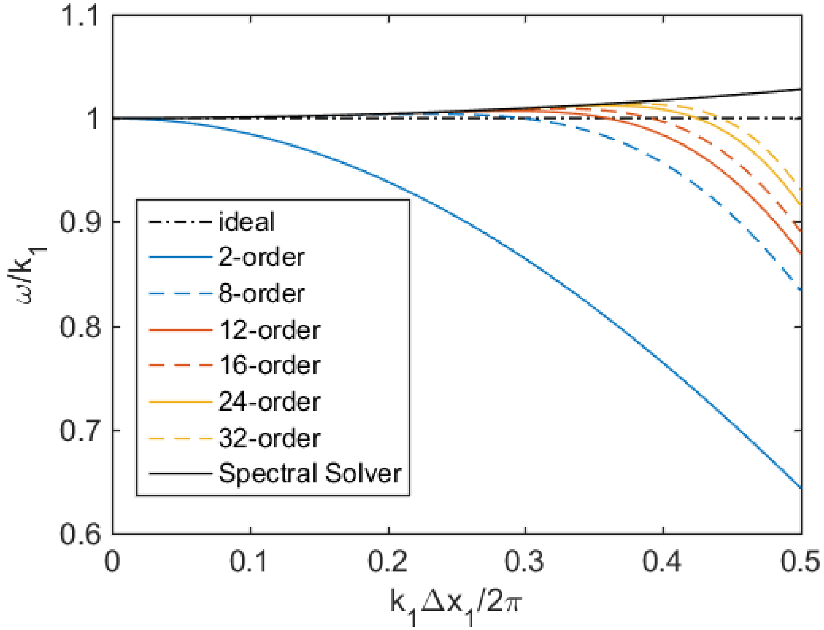


The dispersion curve converges to spectral solver when increasing the solver order *p*.

# NCI modes for HO and FFT based solver

- For high-order and spectral solver, the fastest growing modes (0,0), (0,±1) are highly localized
- The "strip" located at high k range can be readily eliminated by applying a low-pass filter.

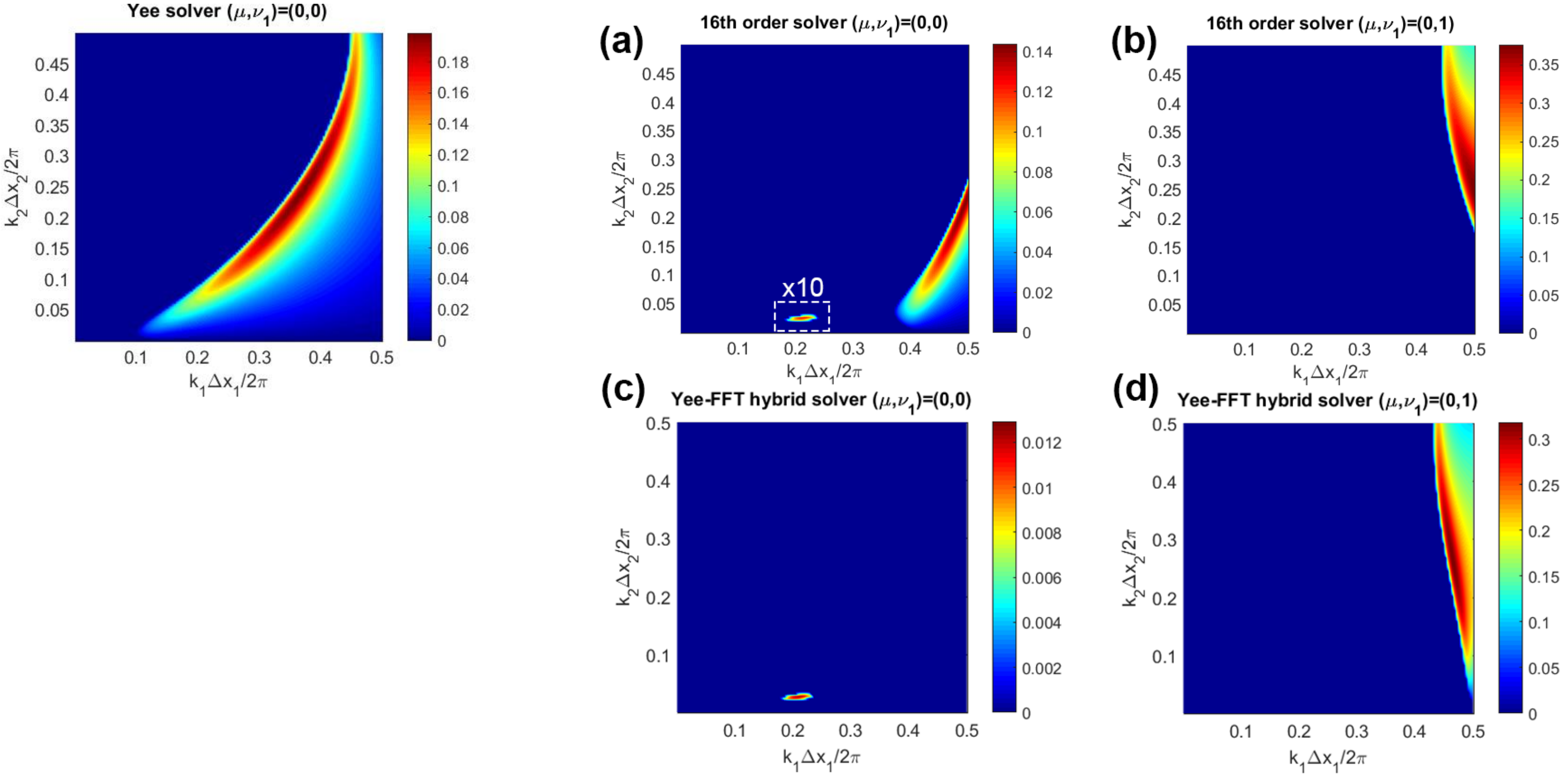

# Customized FDTD solver

- Introducing a slight modification to the [k1](k1) curve where the "dot" resides
- The "bump" can be easily implemented in FFT-based solver
- In HO FDTD solver, one has to find a stencil to match the modified numerical dispersion

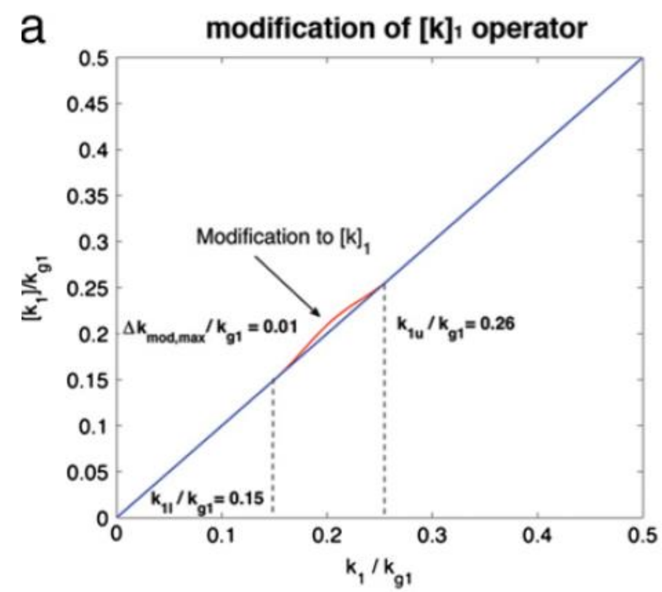


Introduce more solver coefficients to the FDTD stencil

$$[k_1]_p = \sum_{l=1}^{p/2} C_l^p \frac{\sin[(2l-1)k_1\Delta x_1/2]}{\Delta x_1/2} \Longrightarrow [k_1]_{p*} = \sum_{l=1}^{\boxed{M}} \boxed{\tilde{C}_l^p} \frac{\sin[(2l-1)k_1\Delta x_1/2]}{\Delta x_1/2}$$

$$\partial^+_{p*,x_1} f_{i_1,i_2} = \frac{1}{\Delta x_1} \sum_{l=1}^{M} \tilde{C}_l^p \left(f_{i_1+l,i_2} - f_{i_1-l+1,i_2}\right)$$

$$\partial^-_{p*,x_1} f_{i_1,i_2} = \frac{1}{\Delta x_1} \sum_{l=1}^{M} \tilde{C}_l^p \left(f_{i_1+l-1,i_2} - f_{i_1-l,i_2}\right)$$

# Customized FDTD solver

Match the solver coefficients in spirit of constrained least-square method.

Minimize $F_1 = \int_0^{1/2} \left([k_1]_{p*} - [k_1]_p - \Delta k_{\text{mod}}\right)^2 dk_1$ on the contriant $\mathcal{M}\vec{\tilde{C}}^p = \hat{\vec{e}}_1$

where
$\mathcal{M}_{ij} = (2j-1)^{2i-1}/(2i-1)!\ (i = 1, ..., p/2) \text{ and } (j = 1, ..., M)$
$\vec{\tilde{C}}^p = (\tilde{C}_1^p, ..., \tilde{C}_M^p)^T,\ \hat{\vec{e}}_1 = (1, 0, ..., 0)^T$

Reformat into matrix equation

$$\begin{pmatrix} \frac{1}{2\pi^2}\vec{I} & \mathcal{M}^T \\ \mathcal{M} & \vec{0} \end{pmatrix} \begin{pmatrix} \vec{\tilde{C}}^p \\ \vec{\lambda} \end{pmatrix} = \begin{pmatrix} \frac{1}{2\pi^2}(\vec{A} + \vec{C}^p) \\ \hat{\vec{e}}_1 \end{pmatrix}$$

$$A_j = \frac{8\Delta k_{\text{mod,max}}(\cos[(2j-1)\pi k_{1u}] - \cos[(2j-1)\pi k_{1l}])}{(2j-1)[(2j-1)^2(k_{1u} - k_{1l})^2 - 4]}$$

λ： Lagrangian multiplier

# Continuity Equation & Current Correction

- Continuity equation is naturally true for Yee (2nd order) solver
- For HO FDTD solver, current need to be corrected in k-space to make the continuity equation (or Gauss' law) become true

$$
\begin{aligned}
\vec{B}^{n+\frac{1}{2}} &= \vec{B}^{n-\frac{1}{2}} - c\Delta t \nabla_p^{+} \times \vec{E}^{n} \\
\vec{E}^{n+1} &= \vec{E}^{n} + c\Delta t \nabla_p^{-} \times \vec{B}^{n+\frac{1}{2}} - 4\pi \Delta t \vec{J}^{n+\frac{1}{2}}
\end{aligned}
$$

$$\overline{\frac{\partial}{\partial t}}\rho^{n} + \nabla_2^{-} \cdot \vec{J}^{n+\frac{1}{2}} = 0$$

+

Current correction

$$\tilde{J}_1^{n+\frac{1}{2}} = \frac{[k_1]_2}{[k_1]_{p*}} J_1^{n+\frac{1}{2}}$$

$$\overline{\frac{\partial}{\partial t}}\left(-4\pi\rho^{n} + \nabla_{p*}^{-}\vec{E}^{n}\right) = 0$$

# Current Expansion

- Current correction leads to a single particle extending to more cells
- More guard cells are needed to contain the expanded current

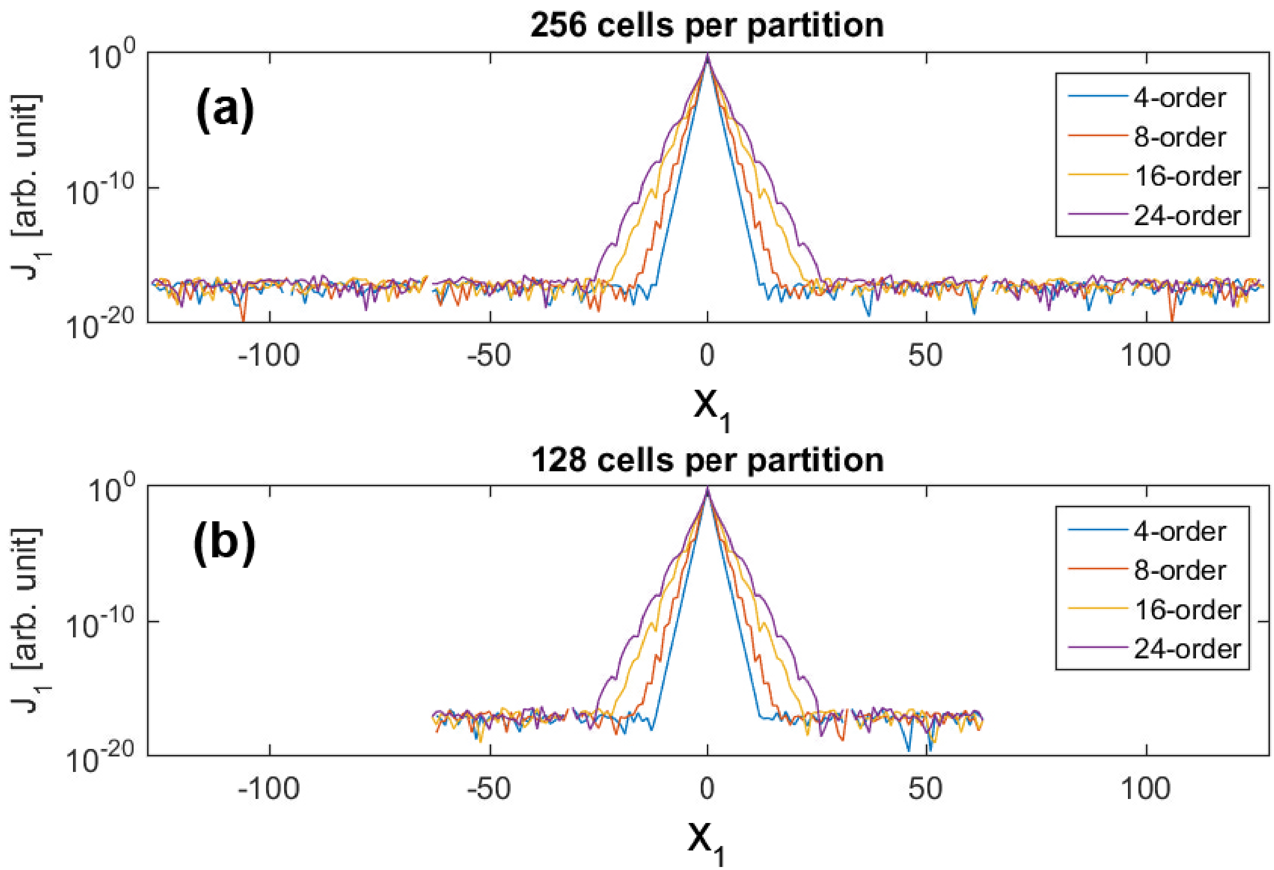

# EM field advance for customized solver

Parallel scalability
- Local FFT. Multiple partitions allowed in plasma drifting direction

Computing efficiency
- FFT/IFFT only performed on current.

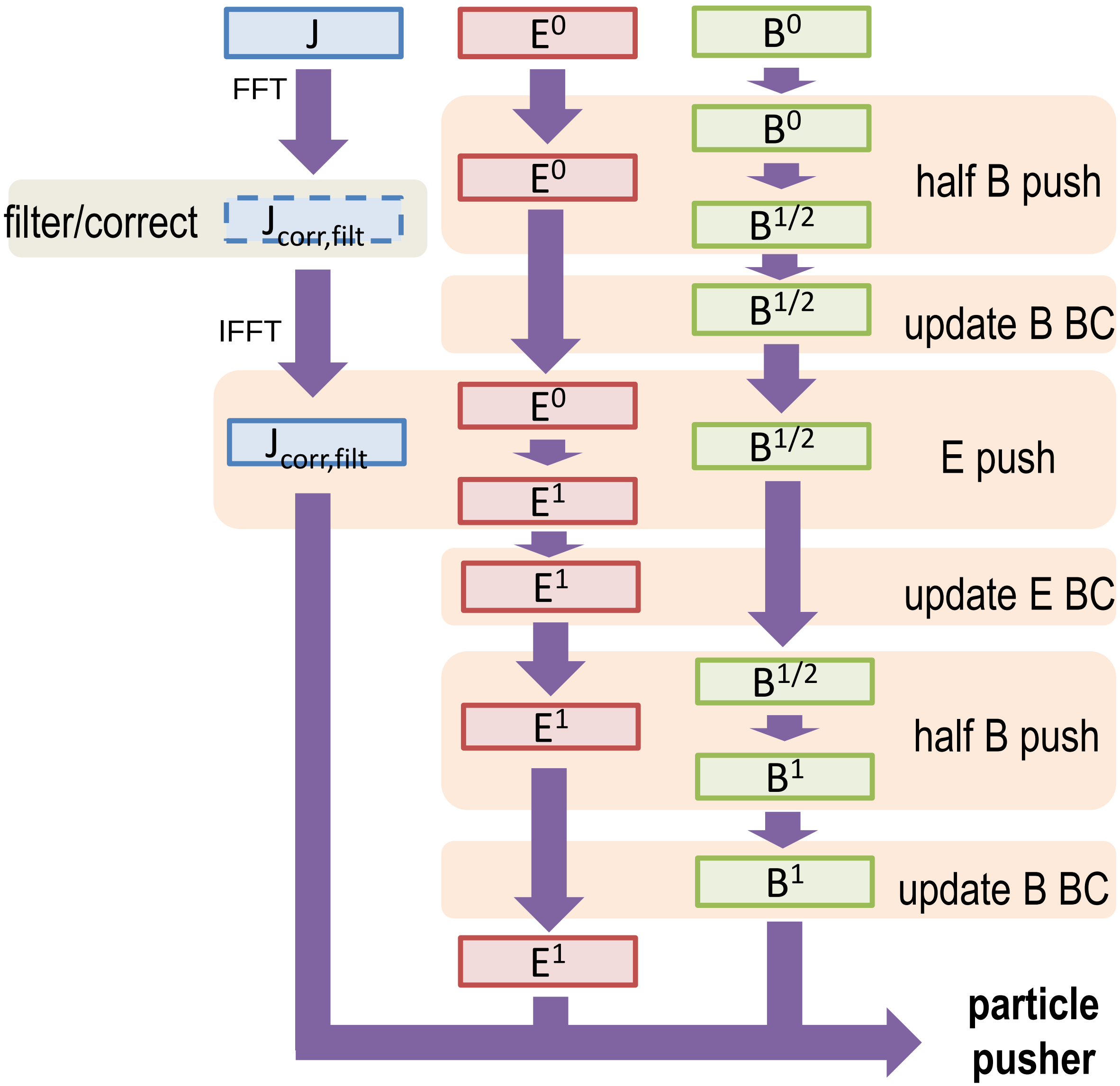


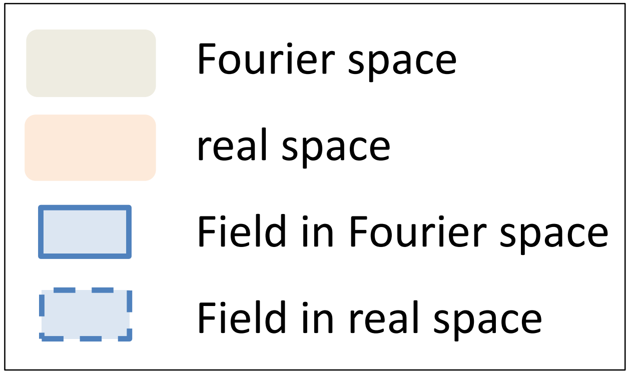

# Example 1: Relativistically drifting plasma

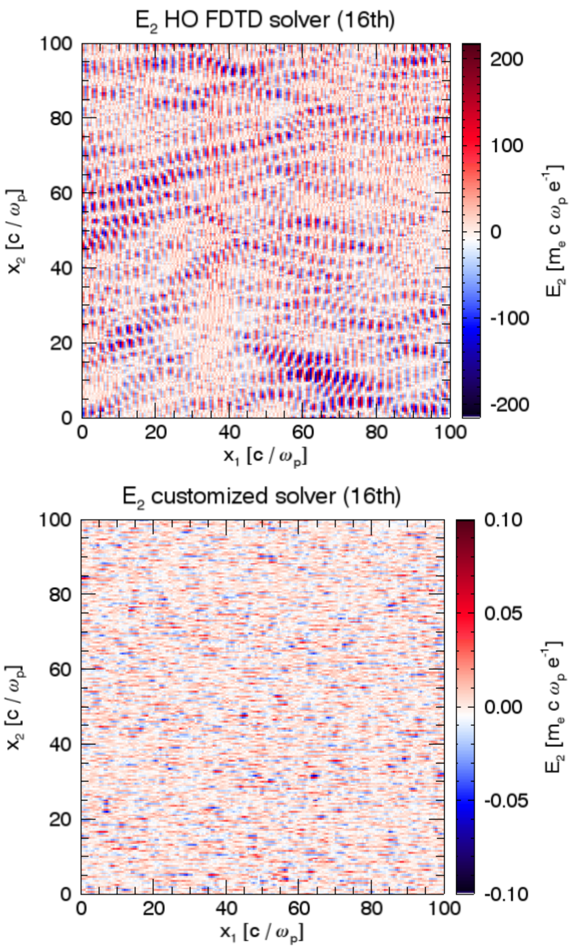


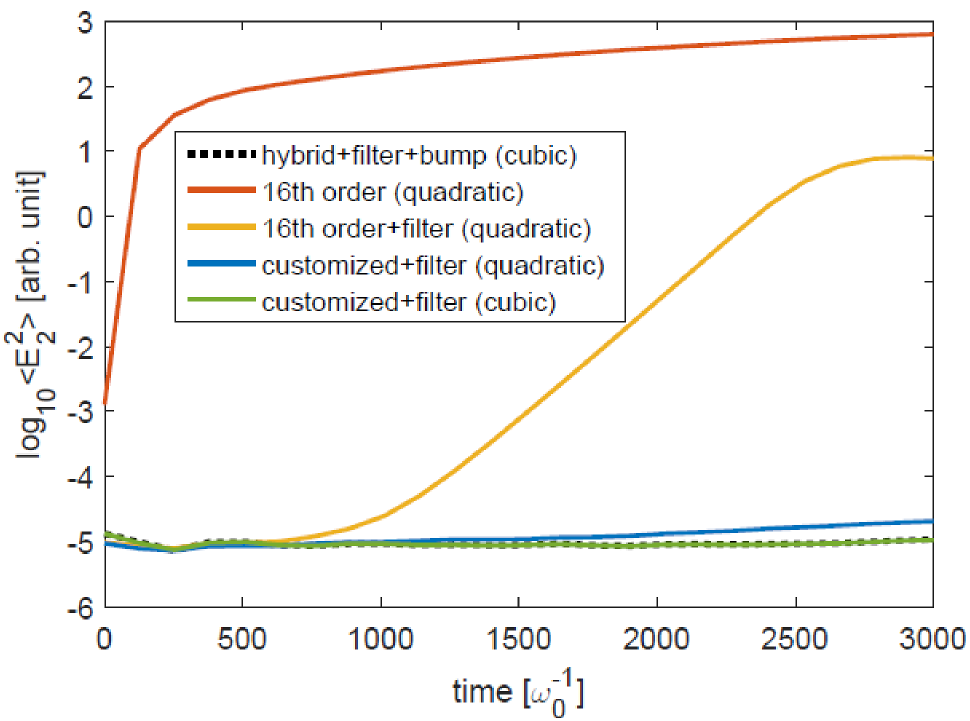


Electric field energy conserves with

**<u>customized FDTD solver + lowpass current filter + cubic particle shape</u>**

# Example 2: LWFA in boosted Lorentz frame

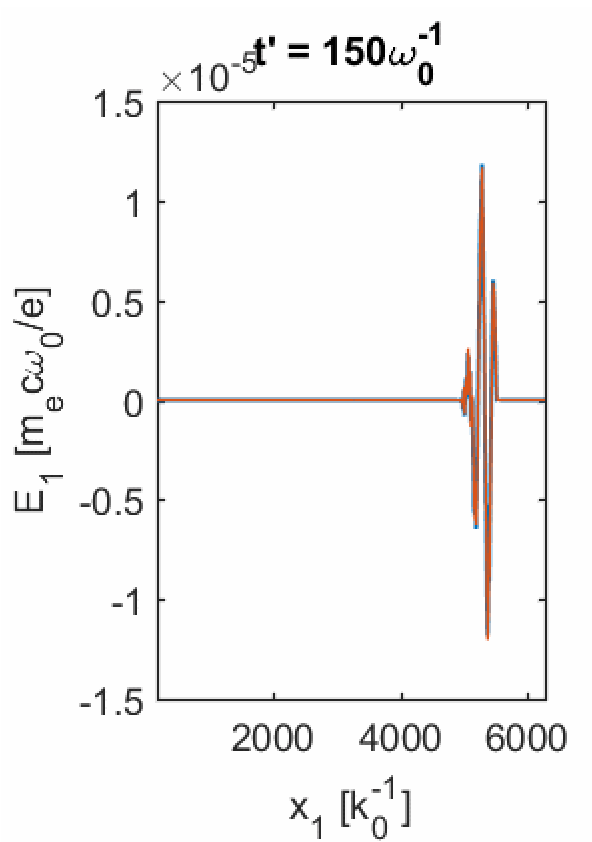


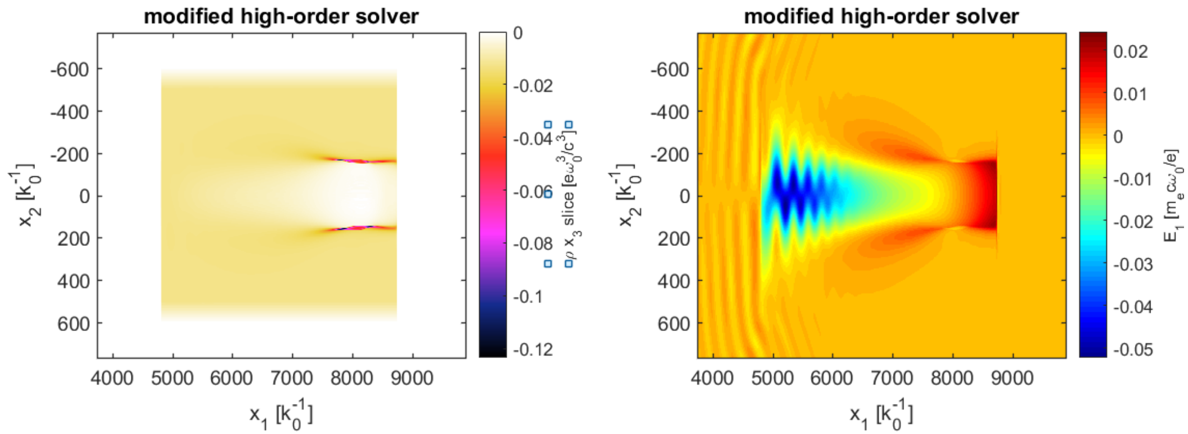


Customized FDTD solver

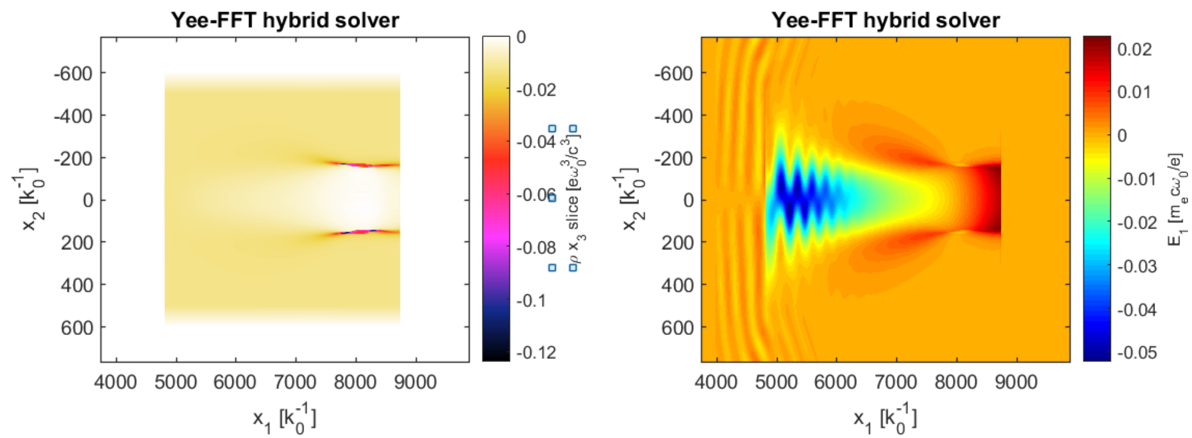


FFT based solver

# Example 3: Beam injection and trapping

Current $I_{peak}$ ~ 10 kA
Energy E ~ 350 MeV

**Slice energy spread**

- Yee solver

~ 15 MeV (NCR modulated)

- Customzed FDTD solver

~1 MeV

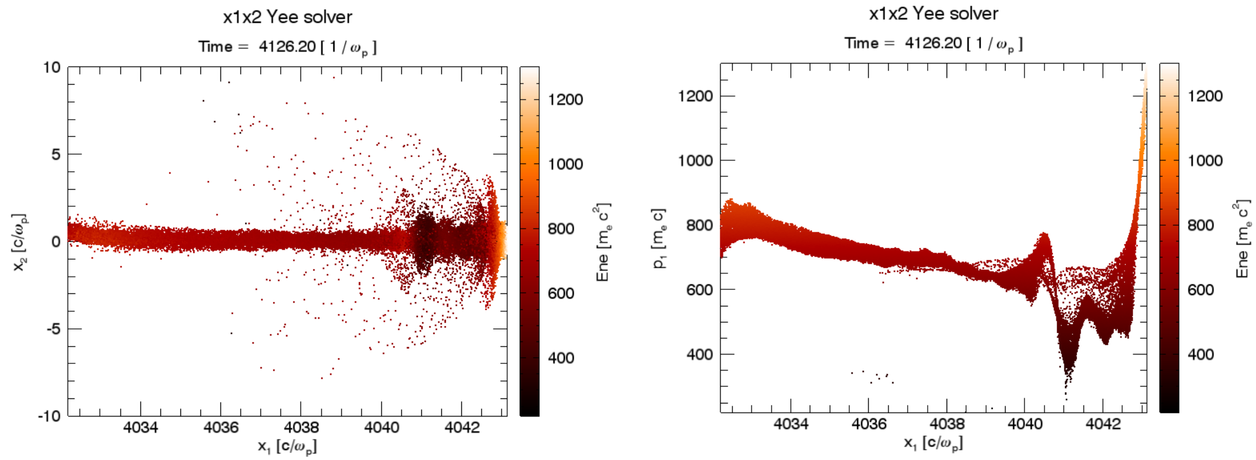


Yee solver

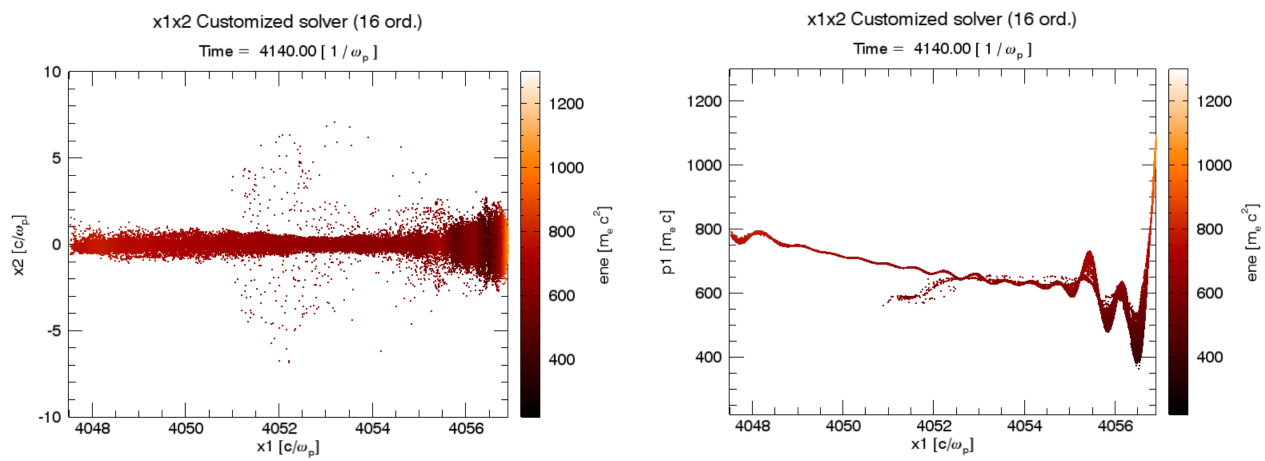


Customized solver ($16^{th}$ order)

**<u>Beam quality (slice energy spread) of injected bunch is greatly improved</u>**

# Tapered High-order FDTD Solver

Linearly increasing the solver order from 2nd to the specified order at the boundary

- Applicable for the Perfect Matched Layer (PML) boundary condition
- Suppressing superluminal numerical noise in moving window simulations

| | | | | | | | | | | | | | |
|---|---|---|---|---|---|---|---|---|---|---|---|---|---|
| 2 | 4 | 6 | 8 | 10 | 12 | 14 | 16 | 16 | 16 | 16 | 16 | 16 | … |
| 2 | 4 | 6 | 8 | 10 | 12 | 14 | 16 | 16 | 16 | 16 | 16 | 16 | … |
| 2 | 4 | 6 | 8 | 10 | 12 | 14 | 16 | 16 | 16 | 16 | 16 | 16 | … |
| 2 | 4 | 6 | 8 | 10 | 12 | 14 | 16 | 16 | 16 | 16 | 16 | 16 | … |
| 2 | 4 | 6 | 8 | 10 | 12 | 14 | 16 | 16 | 16 | 16 | 16 | 16 | … |
| 2 | 4 | 6 | 8 | 10 | 12 | 14 | 16 | 16 | 16 | 16 | 16 | 16 | … |
| 2 | 4 | 6 | 8 | 10 | 12 | 14 | 16 | 16 | 16 | 16 | 16 | 16 | … |
| 2 | 4 | 6 | 8 | 10 | 12 | 14 | 16 | 16 | 16 | 16 | 16 | 16 | … |

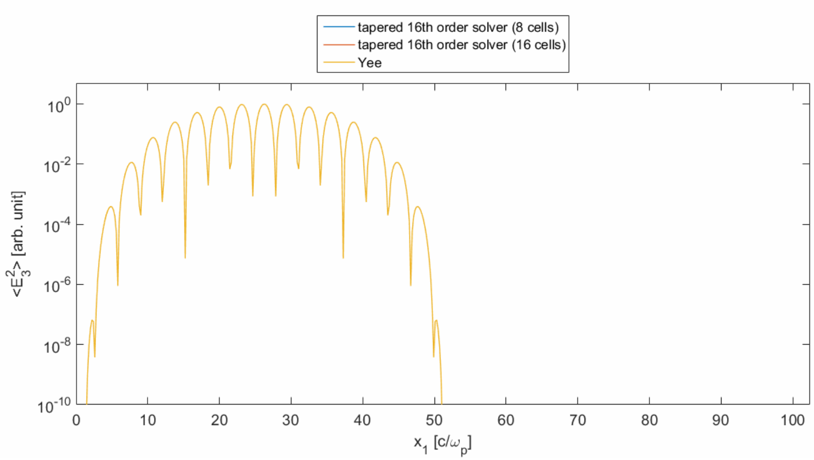


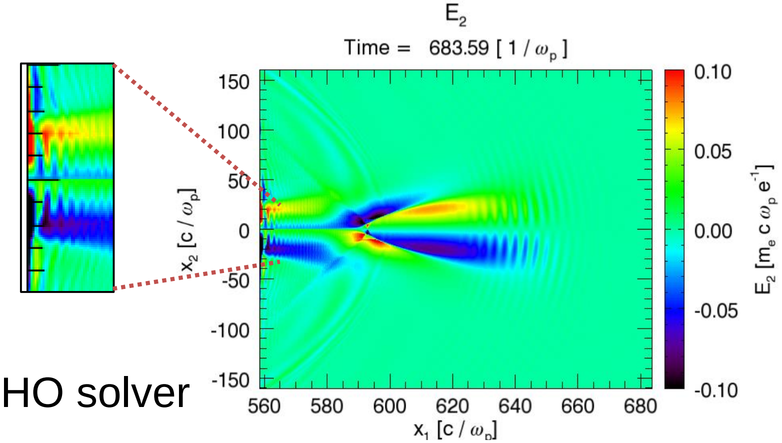


HO solver

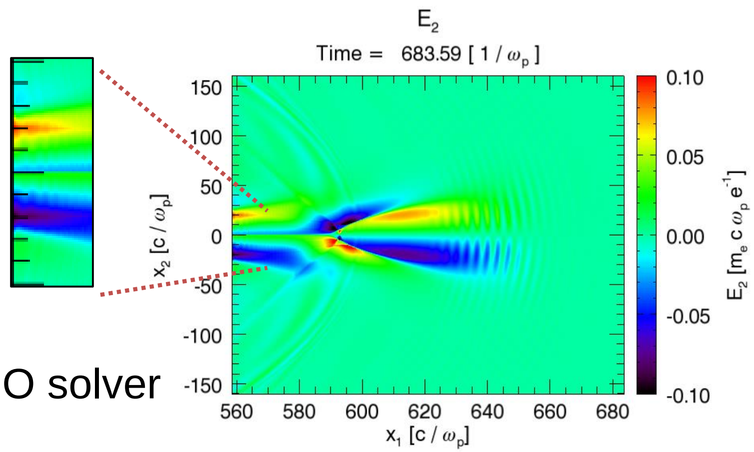


Tapered HO solver

# Summary

- NCI features for HO FDTD Maxwell solver resemble those of FFT-based solver.
- Applying lowpass current filter and bumping the numerical dispersion locally can systematically eliminate the NCI.
- We find a way to customized the solver stencil to achieve the numerical dispersion bumping for HO FDTD solver.
- Customized FDTD solver gains advantage over FFT-based solver on parallel scalability and computing efficiency.

Thanks for your attention!